J|A|C|S
ARTICLES
Published on Web 11/01/2003

Universal NMR Databases for Contiguous Polyols

Shuhei Higashibayashi, Werngard Czechtizky, Yoshihisa Kobayashi, and Yoshito Kishi*

Contribution from the Department of Chemistry and Chemical Biology, Harvard University, 12 Oxford Street, Cambridge, Massachusetts 02138

Received July 25, 2003; E-mail: kishi@chemistry.harvard.edu

Abstract: On the basis of 1,2,3-triols **1a**∼**d**, 1,2,3,4-tetraols **2a**∼**h**, and 1,2,3,4,5-pentaols **3a**∼**p**, NMR databases with four types of profile-descriptors (^{13}C-, ^{1}H-, and ^{1}H(OH)-chemical shifts and vicinal spin-coupling constants) for contiguous polyols are reported. To systematically assess the relative values of these databases, a case study has been conducted on heptaols **4a**∼**d**, through which the γ- and δ-effects have been recognized to refine the ^{13}C and ^{1}H chemical shift profile predicted via an application of the concept of self-contained nature. The magnitudes of γ- and δ-effects depend on a specific stereochemical arrangement of the functional groups present in both the inside and outside of a self-contained box and are significant only for the stereoisomers belonging to a specific sub-group. With the exception of the stereochemical arrangement of functional groups belonging to a specific sub-group, the γ- and δ-effects can, at the first order of approximation, be ignored for the stereochemical analysis of unknown compounds. For the stereoisomers belonging to a specific sub-group, it is necessary to refine, with incorporation of the γ- and δ-effects, the profile predicted at the first order of approximation. With use of heptaols **4a**∼**d**, the values of $^{3}J_{H,H}$ profiles have been assessed. Two methods, one using profiles consisting of three contiguous $^{3}J_{H,H}$ constants and the other using profiles consisting of two contiguous $^{3}J_{H,H}$ constants, have been developed. A stereochemical analysis based on three, or two, contiguous $^{3}J_{H,H}$ profiles is *operationally simpler* than one based on ^{13}C and ^{1}H chemical shift profiles. Therefore, it is recommended to use a $^{3}J_{H,H}$ profile as the primary device to predict the stereochemistry of unknown polyols and ^{13}C and ^{1}H chemical shift profiles as the secondary devices to confirm the predicted stereochemistry.

Introduction

Through the work on palytoxins,[1,2] AAL toxin/fumonisin,[3,4] and maitotoxin,[5,6] we have experimentally demonstrated the following: (1) the spectroscopic profiles of the stereoclusters present in these natural products are inherent to the specific stereochemical arrangement of the small substituents on the carbon backbone and are independent from the rest of the molecules, and (2) steric and stereoelectronic interactions between structural clusters connected either directly or with a one-methylene bridged are significant and interactions between stereoclusters connected with a two- or more-methylene bridge are negligible. On the basis of these experimental discoveries, we have advanced the logic of a universal NMR database approach for assignment of the relative and absolute configuration of (acyclic) compounds. Using the ^{13}C chemical shift profiles as the primary means, we have demonstrated the feasibility and reliability of this approach, which has culminated in the complete stereochemical assignment of the desertomycin/oasomycin class of antibiotics,[7] mycolactone,[8] and tetrafibricin.[9]

(1) (a) Cha, J. K.; Christ, W. J.; Finan, J. M.; Fujioka, H.; Kishi, Y.; Klein. L. L.; Ko, S. S.; Leder, J.; McWhorter, W. W., Jr.; Pfaff, K.-P.; Yonaga, M.; Uemura, D.; Hirata, Y. *J. Am. Chem Soc*. **1982**, *104*, 7369−7371 and the preceding papers. (b) Kishi, Y. *Curr. Trends Org. Synth.* (IUPAC) **1983**, 115−130.

(2) For the stereochemical assignment primarily based on spectroscopic methods, see: Moore, R. E.; Bartolini, G.; Barchi, J.; Bothner-By, A. A.; Dadok, J.; Ford, J. *J. Am. Chem. Soc*. **1982**, *104*, 3776−3779.

(3) For the stereochemical assignment of AAL toxins and fumonisins from this laboratory, see: (a) Boyle, C. D.; Harmange, J.-C.; Kishi, Y. *J. Am. Chem. Soc*. **1994**, *116*, 4995−4996. (b) Boyle, C. D.; Kishi, Y. *Tetrahedron Lett*. **1995**, *36*, 5695−5698, and references therein.

(4) For the work from other laboratories, see: (c) Oikawa, H.; Matsuda, I.; Kagawa, T.; Ichihara, A.; Kohmoto, K. *Tetrahedron* **1994**, *50*, 13 347−13 368. (d) Hoye, T. R.; Jiménez, J. I.; Shier, W. T. *J. Am. Chem. Soc*. **1994**, *116*, 9409−9410. (e) ApSimon, J. W.; Blackwell, B. A.; Edwards, O. E.; Fruchier, A. *Tetrahedron Lett*. **1994**, *35*, 7703−7706. (f) Poch, G. K.; Powell, R. G.; Plattner, R. D.; Weisleder, D. *Tetrahedron Lett*. **1994**, *35*, 7707−7710. (g) Blackwell, B. A.; Edwards, O. E.; ApSimon, J. W.; Fruchier, A. *Tetrahedron Lett*. **1995**, *36*, 1973−1976.

(5) For the work from this laboratory, see: (a) Zheng, W.; DeMattei, J. A.; Wu, J.-P.; Duan, J. J.-W.; Cook, L. R.; Oinuma, H.; Kishi, Y. *J. Am. Chem. Soc*. **1996**, *118*, 7946−7968. (b) Cook, L. R.; Oinuma, H.; Semones, M. A.; Kishi, Y. *J. Am. Chem. Soc*. **1997**, *119*, 7928−7937.

(6) For the work from the laboratories at Tokyo and Tohoku Universities, see: (c) Sasaki, M.; Matsumori, N.; Maruyama, T.; Nonomura, T.; Murata, M.; Tachibana, K.; Yasumoto, T. *Angew. Chem., Int. Ed. Engl*. **1996**, *35*, 1672−1675. (d) Nonomura, T.; Sasaki, M.; Matsumori, N.; Murata, M.; Tachibana, K.; Yasumoto, T. *Angew. Chem., Int. Ed. Engl*. **1996**, *35*, 1675−1678.

(7) (a) Lee, J.; Kobayashi, Y.; Tezuka, K.; Kishi, Y. *Org. Lett*. **1999**, *1*, 2177−2180. (b) Kobayashi, Y.; Lee, J.; Tezuka, K.; Kishi, Y. *Org. Lett*. **1999**, *1*, 2181−2184. (c) Kobayashi, Y.; Tan, C.-H.; Kishi, Y. *Helv. Chim. Acta* **2000**, *83*, 2562−2571. (d) Kobayashi, Y.; Tan. C.-H.; Kishi, Y. *Angew. Chem., Int. Ed*. **2000**, *39*, 4279−4281. (e) Tan. C.-H.; Kobayashi, Y.; Kishi, Y. *Angew. Chem., Int. Ed*. **2000**, *39*, 4282−4284. (f) Kobayashi, Y.; Hayashi, N.; Tan. C.-H.; Kishi, Y. *Org. Lett*. **2001**, *3*, 2245−2248. (g) Hayashi, N.; Kobayashi, Y.; Kishi, Y. *Org. Lett*. **2001**, *3*, 2249−2252. (h) Kobayashi, Y.; Hayashi, N.; Kishi, Y. *Org. Lett*. **2001**, *3*, 2253−2255. (i) Kobayashi, Y.; Tan. C.-H.; Kishi, Y. *J. Am. Chem. Soc*. **2001**, *123*, 2076−2078. (j) Kobayashi, Y.; Hayashi, N.; Kishi, Y. *Org. Lett*. **2002**, *4*, 411−414.

(8) (a) Benowitz, A. B.; Fidanze, S.; Small, P. L.; Kishi, Y. *J. Am. Chem. Soc*. **2001**, *123*, 5128−5129. (b) Fidanze, S.; Song, F.; Szlosek-Pinaud, M.; Small, P. L.; Kishi, Y. *J. Am. Chem. Soc*. **2001**, *123*, 10 117−10 118.

(9) Kobayashi, Y.; Czechtizky, W.; Kishi, Y. *Org. Lett.* **2003**, *5*, 93−96.

10.1021/ja0375481 CCC: $25.00

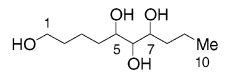

	C5	C6	C7
1a	α	α	α
1b	α	β	α
1c	α	α	β
1d	α	β	β

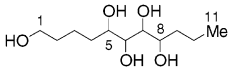

	C5	C6	C7	C8
2a	α	α	α	α
2b	β	α	β	α
2c	β	α	α	β
2d	α	α	β	β

	C5	C6	C7	C8
2e	α	α	α	β
2f	β	α	α	α
2g	α	α	β	α
2h	β	α	β	β

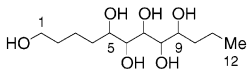

	C5	C6	C7	C8	C9
3a	α	α	α	α	α
3b	β	α	β	α	β
3c	β	α	α	α	β
3d	α	α	β	α	α
3e	α	α	α	α	β
3f	β	α	α	α	α
3g	α	α	α	β	α
3h	β	α	β	β	β

	C5	C6	C7	C8	C9
3i	α	α	α	β	β
3j	α	α	β	β	β
3k	α	α	β	β	α
3l	β	α	α	β	β
3m	α	α	β	α	β
3n	β	α	β	α	α
3o	β	α	α	β	α
3p	β	α	β	β	α

Figure 1. NMR Database substrates used for the 1,2,3-triol (**1a**∼**d**), 1,2,3,4-tetraol (**2a**∼**h**), and 1,2,3,4,5-pentaol (**3a**∼**p**) systems.

Needless to point out, spectroscopic profiles can be described by other parameters such as vicinal $^1H/^1H$ spin-coupling ($^3J_{H,H}$) constants. In this paper, we will report the $^3J_{H,H}$ databases, as well as the ^{13}C, ^1H, and ^1H(OH) chemical shift databases, for contiguous polyols, which allows us for the first time to systematically compare the values of each of the NMR databases using different descriptors.

Synthesis and Stereochemical Assignment of NMR Database Polyols. We chose, and synthesized, **1a**∼**d**, **2a**∼**h**, and **3a**∼**p** as the substrates to create the NMR database for 1,2,3-triols, 1,2,3,4-tetraols, and 1,2,3,4,5-pentaols, respectively. To correlate directly with previously created NMR databases, these database substrates were designed to share the same structural moiety at the left- and right-terminals with the database compounds previously used.

The 1,2,3-triols **1a**∼**d** were synthesized in an optically active form from the chiral propargyl alcohol **A** (Scheme 1).[10,11] Using the procedures well precedented in the literature, i.e., LAH and H_2/Lindlar-catalyst, **A** was selectively reduced to *trans*- and *cis*-allylic alcohols **B-1** and **B-2**, respectively. The spin-coupling constants observed for the olefinic protons confirmed the stereochemistry of **B-1** and **B-2**. After benzylation, **B-1** and **B-2** were subjected to OsO_4-dihydroxylation, to furnish a 3:1 mixture of *threo*-products and a 9:1 mixture of *erythro*-products, respectively, which were effectively separated by silica gel chromatography. Thus, 1,2,3-triols **1a**∼**d** were obtained in a stereochemically homogeneous form and fully characterized.

Scheme 1

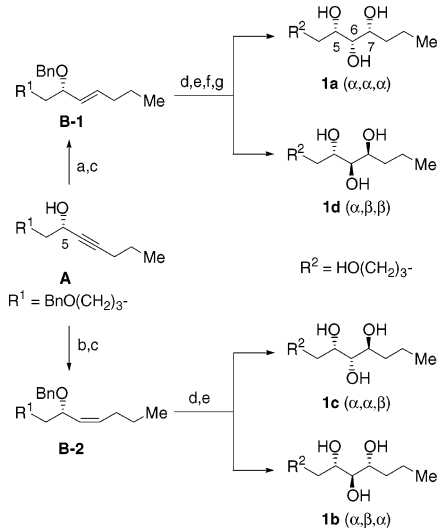

Reagents and Reaction Conditions (a) $LiAlH_4$, THF, rt. (b) H_2, Lindlar catalyst, quinoline, hexane, rt. (c) NaH, BnBr, $(n\text{-}Bu)_4NI$, DMF, rt. (d) OsO_4, NMO, acetone/H_2O, rt. (e) H_2, Pd-on-C, MeOH, rt. (f) Ac_2O, pyridine, rt. (g) NaOMe, MeOH, rt.

The stereochemistry of 1,2,3-triols **1a**∼**d** was assigned for the following reason. The major triol derived from *trans*-allylic alcohol **B-1** should correspond to either **1a** or **1d**, whereas the major triol derived from *cis*-allylic alcohol **B-2** should correspond to either **1c** or **1b**. On the basis of the empirical rule,[12] we predicted that the major diastereomer obtained from *trans*- and *cis*-allylic alcohols **B-1** and **B-2** corresponds to **1d** and **1b**, respectively. This assignment was further supported by NMR spectroscopy. Ignoring the difference in structure at the two terminal positions, we recognized the presence of a plane of symmetry for **1a** and **1b** but not for **1d** and **1c**. Indeed, this was well reflected in their ^1H [**1a**: 3.64 ppm (H5, H7), 3.20 (H6); **1b**: 3.59 (H5, H7), 3.29 (H6); **1c**: 3.81 (H5), 3.15 (H6), 3.61 (H7); **1d**: 3.59 (H5), 3.15 (H6), 3.82 (H7)] and ^{13}C [**1a**: 73.5 ppm (C5), 76.7 (C6), 73.3 (C7); **1b**: 74.0 (C5), 78.3 (C6), 73.8 (C7); **1c**: 71.5 (C5), 76.9 (C6), 72.6 (C7); **1d**: 72.7 (C5), 76.9 (C6), 71.1 (C7)] NMR spectra in CD_3OD.

The 1,2,3,4-tetraols **2a**∼**h** were synthesized in an optically active form from D-pentoses (Scheme 2).[13] In this synthesis, the C6,C7,C8-stereochemistry of **2a**∼**h** was predetermined by D-pentoses used. The left-side chain was introduced via a Grignard reaction to yield the expected product as a diastereomeric mixture at C5. After benzylation, the mixture was separated by silica gel chromatography (Biotage), to furnish the stereochemically homogeneous C5 diastereomers. Thus, all the required 1,2,3,4-triols **2a**∼**h** were obtained in a stereochemically homogeneous form and fully characterized.

The C5-stereochemistry was assigned as follows: Ignoring the difference in structure at the termini, we noticed that one of

(10) The optically active propargyl alcohol **A** was prepared, following the protocol reported by T. Oriyama: Sano, T.; Imai, K.; Ohashi, K.; Oriyama, T. *Chem. Lett*. **1999**, *3*, 265−266.

(11) The synthesis outlined in Scheme 1 was carried out with the antipode of **A**.

(12) (a) Christ, W. J.; Cha, J. K.; Kishi, Y. *Tetrahedron Lett.* **1983**, *24*, 3947−50. (b) Cha, J. K.; Christ, W. J.; Kishi, Y. *Tetrahedron* **1984**, *40*, 2247−55.

(13) Tribenzyl D-xylopyranose, tribenzyl D-arabinopyranose, tribenzyl D-ribopyranose, and tribenzyl D-lyxopyranose were prepared by the method reported: (a) tribenzyl D-xylopyranose: Tsuda, Y.; Nunozawa, T.; Yoshimoto, K. *Chem. Pharm. Bull.* **1980**, *28*, 3223−3231. (b) tribenzyl *D*-arabinopyranose: Mizutani, K.; Ohtani, K.; Kasai, R.; Tanaka, O.; Matsuura, H. *Chem. Pharm. Bull.* **1985**, *33*, 2266−2272. (c) tribenzyl *D*-ribopyranose: Tejima, S.; Ness, R. K.; Kaufman, R. L.; Fletcher, H. G. Jr. *Carbohydr. Res.* **1968**, *7*, 485−490. (d) tribenzyl D-lyxopyranose: Dhawan, S. N.; Chick, T. L.; Goux, W. J. *Carbohydr. Res.* **1988**, *172*, 297−307; Gigg, R,; Warren, C. D. *J. Chem. Soc.* **1965**, 2205−2210.

Scheme 2

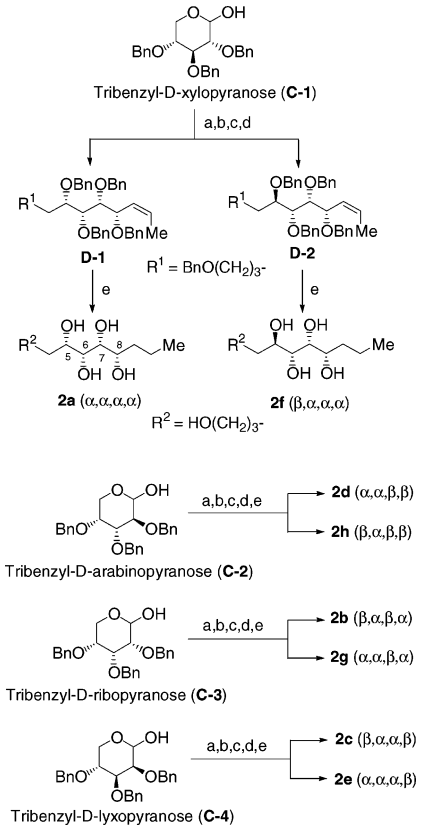

Reagents and Reaction Conditions (a) KHMDS, $(Ph)_3P^+CH_2CH_3I^-$, THF, 0 °C to room temperature. (b) $(COCl)_2$, DMSO, CH_2Cl_2, −78 °C, then NEt_3, −78 °C to room temperature. (c) $BnO(CH_2)_4MgBr$, THF or Et_2O, 0 °C. (d) NaH, BnBr, $(n\text{-}Bu)_4N^+I^-$, DMF, rt. (e) H_2, $Pd(OH)_2$, EtOH/EtOAc.

the two diastereomers formed in each series contains a symmetry element, which was clearly detected in its NMR spectra. For example, one of the tetraols derived from xylose gave the ^1H [3.70 ppm (H5, H8), 3.49 (H6, H7)] and ^{13}C [73.0 ppm (C5), 75.3 (C6, C7), 72.7 (C8)] NMR spectra in CD_3OD, whereas the other gave the ^1H [3.62 ppm (H5), 3.37 (H6), 3.65 (H7), 3.66 (H8)] and ^{13}C [72.5 (C5), 76.2 (C6), 73.3 (C7), 74.3 (C8)] NMR spectra. This spectroscopic observation allowed us to assign **2a** and **2f** to the former and latter diastereomers, respectively. Similarly, the stereochemistry was assigned for the tetraols derived from arabinose, ribose, and lyxose.

The 1,2,3,4,5-pentaols **3a**∼**p** were synthesized in an optically active form from the synthetic intermediates used in the 1,2,3,4-tetraol syntheses (Scheme 3). In this synthesis, the right-side chain was introduced via a Grignard reaction, to yield the expected product as a diastereomeric mixture at C9. Silica gel chromatography (Biotage) was effective to obtain all the 1,2,3,4,5-pentaols **3a**∼**p** in a stereochemically homogeneous form and fully characterized.

Using the same logic as the one used in the 1,2,3,4-tetraol series, we assigned the C9-stereochemistry for the diastereomers formed in the Grignard reaction for each series. In the **D-1**, **D-2**, **D-5**, and **D-6** series, one of the two C9-diastereomers contains a (pseudo)symmetry element which was clearly detected by NMR spectroscopy. In the remaining four series, neither of the C9-diastereomers have a (pseudo)symmetry element. Ignoring the difference in structure at the termini, we noticed that one of the C9-diastereomers formed in these series is identical to one

Scheme 3

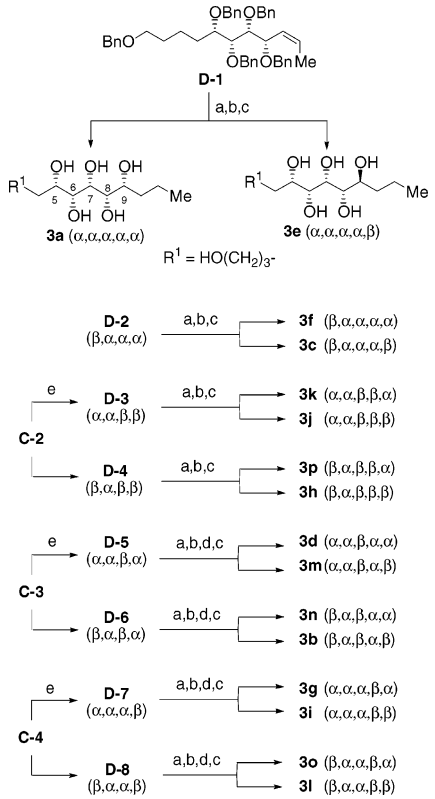

Reagents and Reaction Conditions (a) O_3, AcONa, $MeOH/CH_2Cl_2$, −78 °C, then DMS, rt. (b) $CH_3(CH_2)_2MgBr$, THF or Et_2O, 0 °C. (c) H_2, $Pd(OH)_2$, EtOH/EtOAc. (d) NaH, BnBr, $(n\text{-}Bu)_4N^+I^-$, DMF, rt. (e) See Scheme 2.

of the C9-diastereomers formed in the other series and consequently they should exhibit (almost) identical NMR properties. Using this logic, we could assign the stereochemistry to all the 1,2,3,4,5-pentaols **3a**∼**p**.

NMR Databases.

a. Carbon Chemical Shift Database. The ^{13}C chemical shifts were measured in three solvents [CD_3OD, $(CD_3)_2SO$, D_2O] for each diastereomer of **1a**∼**d**, **2a**∼**h**, and **3a**∼**p**. Following the previous procedure,[7] their ^{13}C chemical shift databases were then created. For all three polyol series, the ^{13}C chemical shift databases in CD_3OD and $(CD_3)_2SO$ were found to be very similar to each other. However, the overall ^{13}C chemical shift profiles in D_2O were found to be similar to those in CD_3OD and $(CD_3)_2SO$, but some differences in the magnitude of $\Delta\delta$'s as well as the pattern of profiles were noticed. For illustration, we show the ^{13}C chemical shift profiles of **1a**∼**d** in CD_3OD, $(CD_3)_2SO$, and D_2O (Chart 1) and the ^{13}C chemical shift profiles of **2a**∼**h** and **3a**∼**p** in CD_3OD only (Chart 2). Among the three solvents tested, we slightly prefer CD_3OD to $(CD_3)_2SO$ or D_2O, considering the magnitude of $\Delta\delta$'s and the vicinal $^1H/^1H$ spin-coupling ($^3J_{H,H}$) profiles (vide infra). The complete ^{13}C chemical shift profiles are given in Supporting Information.

b. Proton Chemical Shift Database. The ^1H chemical shifts were measured in three solvents [CD_3OD, $(CD_3)_2SO$, D_2O] for each diastereomer of **1a**∼**d**, **2a**∼**h**, and **3a**∼**p**. Following the procedure used for the ^{13}C chemical shifts, the ^1H chemical shift profiles were created. The overall trends found in ^1H chemical shift profiles are amazingly parallel to those found in the ^{13}C chemical shift profiles, including the following: (1) the ^1H chemical shift profiles in CD_3OD and $(CD_3)_2SO$ are very similar

Chart 1. Difference in ^{13}C Chemical Shifts (100 MHz) between the Average and the Values of **1a**∼**d** in CD_3OD (Panel A), $((CD_3)_2SO$ (Panel B), and D_2O (Panel C)[a]

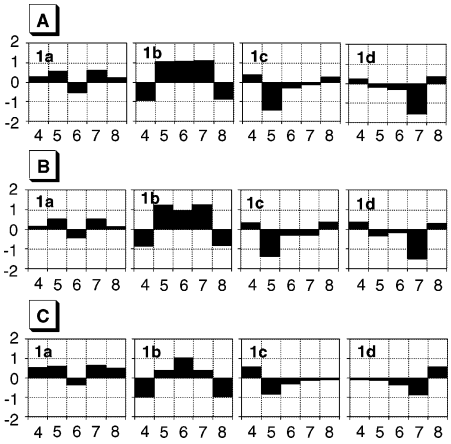

[a] The *x* and *y* axes represent carbon number and $\Delta\delta = \delta_{1a\sim d} - \delta_{ave}$ in ppm, respectively.

Chart 2. Difference in ^{13}C Chemical Shifts (100 MHz) between the Average and the Values of Triols **1a**∼**d** (Panel A), Tetraols **2a**∼**h** (Panel B), and Pentaols **3a**∼**p** (Panel C) in CD_3OD[a]

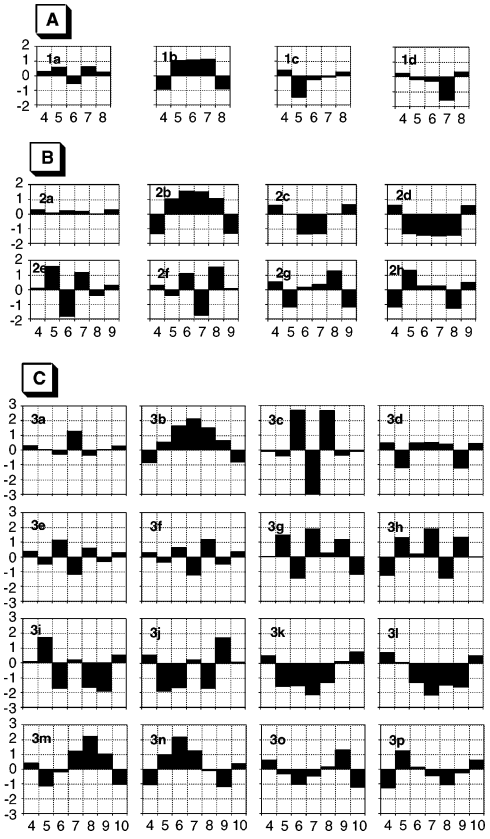

[a] The *x* and *y* axes represent carbon number and $\Delta\delta = \delta_{each\ sub} - \delta_{ave}$ in ppm, respectively.

each other and (2) the ^1H chemical shift profiles in D_2O are similar to those in CD_3OD and $(CD_3)_2SO$, but some differences in the magnitude of $\Delta\delta$'s as well as the pattern of profiles are noticeable. Charts 3 and 4 show the ^1H chemical shift profiles of **1a**∼**d** in CD_3OD, $(CD_3)_2SO$, and D_2O and the ^1H chemical shift profiles of **2a**∼**h** and **3a**∼**p** in CD_3OD only. The complete ^1H chemical shift profiles are given in Supporting Information.

Chart 3. Difference in ^1H Chemical Shifts (500 MHz) between the Average and the Values of **1a**∼**d** in CD_3OD (Panel A), $(CD_3)_2SO$ (Panel B), and D_2O (Panel C)[a]

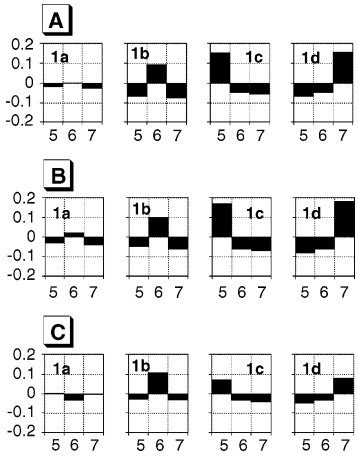

[a] The *x* and *y* axes represent proton number and $\Delta\delta = \delta_{1a\sim d} - \delta_{ave}$ in ppm, respectively.

c. Hydroxy-Proton Chemical Shift Database. During data-collection for the ^1H chemical shift databases, we noticed the following: (1) all the hydroxy-protons give a sharp resonance in $(CD_3)_2SO$; (2) a chemical shift observed for each hydroxy-proton differs from others; (3) the chemical shift for a given hydroxy-proton is not concentration-dependent at $[C] = 1.6 \times 10^2$, 1.6×10, and 1.6 mM. Following the same procedure as before, the hydroxy-proton chemical shift profiles, referred to as a ^1H(OH) chemical shift NMR database, were created for 1,2,3-triols **1a**∼**d**, 1,2,3,4-tetraols **2a**∼**h**, and 1,2,3,4,5-pentaols **3a**∼**p** (Chart 5). Although their potentials are not fully exploited yet, we believe that the ^1H(OH) chemical shift NMR database should become an additional means, possibly complementary to the ^{13}C and ^1H chemical shift NMR databases, for stereochemical analysis of unknown compounds.

d. Vicinal $^1H/^1H$ Spin-Coupling Database. Thus far, we have focused on the NMR databases whose profiles are described by ^{13}C and ^1H chemical shifts. Obviously, some other parameters could be used for profiling NMR characteristics, and we have been curious to explore the potential that the vicinal $^1H/^1H$ spin-coupling ($^3J_{H,H}$) constants offer for the universal database approach. In this context, the contiguous polyol NMR database compounds such as **1a**∼**d**, **2a**∼**h**, and **3a**∼**p** should provide us with an ideal testing ground.

The apparent $^3J_{H,H}$ constants were extracted from 1D ^1H NMR spectra and presented in the form of a bar graph. It should be noted that an experimentally observed $^3J_{H,H}$ constant is directly used in the $^3J_{H,H}$ profiles, whereas a deviation of an experimentally observed chemical shift from the averaged chemical shift for a given nucleus is used for ^{13}C and ^1H chemical shift profiles. Three solvents CD_3OD, $(CD_3)_2SO$, and D_2O were tested for all the substrates; well-defined $^3J_{H,H}$ constants were observed in CD_3OD and D_2O, but accurate $^3J_{H,H}$ constants in $(CD_3)_2SO$ were difficult to determine due to serious signal-broadenings. Later, pyridine-d_5 was also found to be an excellent solvent for this purpose.

Interestingly, both overall profiles and $^3J_{H,H}$ constants in CD_3OD, pyridine-d_5, and D_2O were found to be almost identical. For illustration, Charts 6 and 7 show the $^3J_{H,H}$ profiles of **1a**∼**d** in CD_3OD, D_2O, and pyridine-d_5, and the $^3J_{H,H}$ profiles of **2a**∼**h**

Chart 4. Difference in ^{1}H Chemical Shifts (500 MHz) between the Average and the Values of Triols **1a**∼**d** (Panel A), Tetraols **2a**∼**h** (Panel B), and Pentaols **3a**∼**p** (Panel C) in CD_3OD[a]

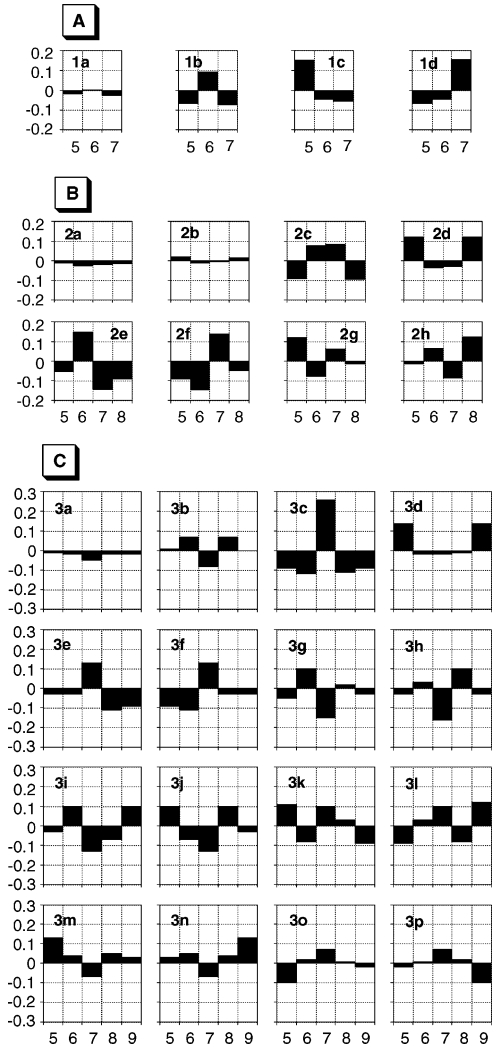

[a] The *x* and *y* axes represent proton number and $\Delta\delta = \delta_{\text{each sub}} - \delta_{\text{ave}}$ in ppm, respectively.

Chart 5. Difference in Hydroxy-^{1}H Chemical Shifts (500 MHz) between the Average and the Values of Triols **1a**∼**d** (Panel A), Tetraols **2a**∼**h** (Panel B), and Pentaols **3a**∼**p** (Panel C) in $((CD_3)_2SO$[a]

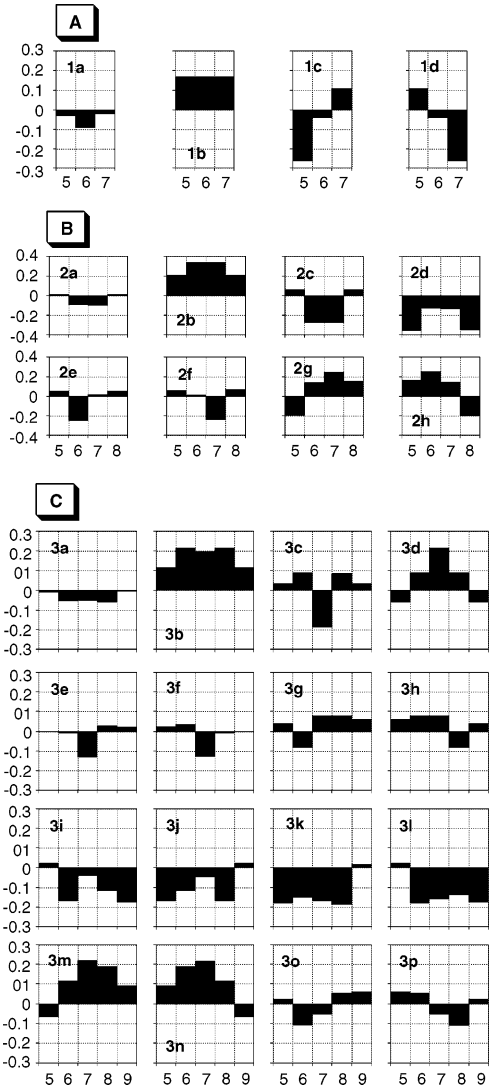

[a] The *x* and *y* axes represent proton number and $\Delta\delta = \delta_{\text{each sub}} - \delta_{\text{ave}}$ in ppm, respectively.

and **3a**∼**p** in CD_3OD, respectively. The complete $^3J_{H,H}$ profiles are included in Supporting Information.

Analysis of NMR Databases. To develop the NMR database approach for the stereochemical assignment of unknown compounds, we have used the ^{13}C chemical shift profile as the primary vehicle to demonstrate its feasibility, reliability, and applicability.[7] In the present work, we have created the ^{13}C, ^{1}H, and ^{1}H(OH) chemical shift databases, as well as the $^3J_{H,H}$ databases, for contiguous polyols, which allows us to systematically compare for the first time the values of each of the NMR databases using different descriptors.

As seen from Charts 1∼7, each diastereomer of **1a**∼**d**, **2a**∼**h**, and **3a**∼**p** exhibits a distinct and differing profile in all the ^{13}C, ^{1}H, ^{1}H(OH), and $^3J_{H,H}$ NMR databases for the 1,2,3-triol-, 1,2,3,4-tetraol-, and 1,2,3,4,5-pentaol-systems. Therefore, any one of these NMR databases can be used for stereochemical analysis of unknown compounds bearing these structural motifs.

The NMR database approach has been founded on the hypothesis, and experimental observations supporting this hypothesis, that the structural properties of a compound in question are as follows: (1) inherent to the specific stereochemical arrangements of (small) substituents on its carbon backbone and (2) independent from the rest of the molecule.[5,7] Thus, we expect that the substrates bearing the same structural motif should exhibit an (almost) identical profile. This trend is indeed recognized in three ways. First, ignoring the difference in structure at the termini, one notices that **1a**,**b** in the triol series, **2a**∼**d** in the tetraol series, and **3a**∼**d** in the pentaol series contain a symmetry element and therefore expects that they should exhibit an NMR profile with a symmetrical nature. Indeed, a beautifully symmetrical pattern is recognized in all the ^{13}C, ^{1}H, ^{1}H(OH), and $^3J_{H,H}$ NMR profiles. Second, ignoring the difference in structure at the termini, one notices that the pair of **1c**/**1d** in the triol series, the pairs of **2e**/**2f** and **2g**/**2h** in the tetraol series, and the pairs of **3e**/**3f**, **3g**/**3h**, **3i**/**3j**, **3k**/**3l**, **3m**/**3n**, and **3o**/**3p** in the pentaol series contain the stereoclusters with a same relative stereochemistry in an opposite direction and therefore expects that these pairs should have the mirror images of

Chart 6. Vicincal $^1H/^1H$ Spin-Coupling Constants of **1a**∼**d** in CD_3OD (Panel A), C_5D_5N (Panel B), and D_2O (Panel C)[a]

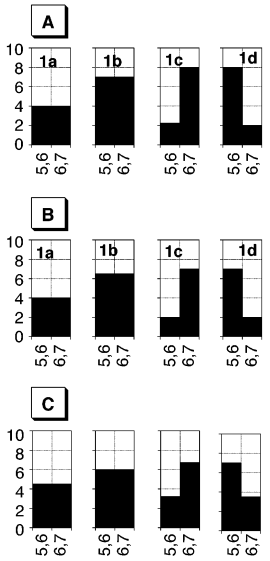

[a] The *x* and *y* axes represent proton number and the $^3J_{H,H}$ constant in Hz, respectively.

(almost) identical NMR profiles. Indeed, it is the case for all the ^{13}C, ^1H, $^1H(OH)$, and $^3J_{H,H}$ NMR profiles observed for these pairs. Third, one notices that the stereoclusters in the higher polyol series contain the stereoclusters in the lower series and therefore expects that the NMR profile found in the lower polyol series should be inherited in the stereoclusters in the higher polyol series. Due to the additional functional group(s) present within a stereocluster in the higher polyol series, the NMR profile of the lower polyol series may be distortedly inherited to the higher polyol series.[7] Nevertheless, this trend is recognizable; for example, the C5∼C8 stereocluster of **3h** and **3p**, as well as the C9∼C6 stereocluster of **3g** and **3o**, corresponds to the C5∼C8 stereocluster of **2h** and the characteristics in the NMR profiles of **2h** are indeed noticeable in the relevant portions of the NMR profile of **3h** and **3p**, as well as **3g** and **3o**.

These characteristics recognized in the ^{13}C, ^1H, $^1H(OH)$, and $^3J_{H,H}$ NMR profiles argue for the usefulness of these NMR databases for predicting the stereochemistry of unknown compounds bearing a relevant structural motif. As will be discussed in the following section, among them, the $^3J_{H,H}$ database provides us with the *operationally simplest* device for analysis of the stereochemistry of unknown contiguous polyols.

Application of NMR Databases for Stereochemical Assignment of Unknown Contiguous Polyols.

a. Carbon Chemical Shift NMR Database. The ^{13}C chemical shift NMR databases created for the 1,2,3-triol, 1,2,3,4-tetraol, and 1,2,3,4,5-pentaol systems can be used for the stereochemical assignments of unknown compounds bearing these structural motifs. For their applications, several guidelines are in order.

As stated in the previous work, steric and/or stereoelectronic interactions between the structural motifs connected either directly or with a one-bridging carbon are significant, whereas interactions between the structural motifs connected with two- or more-bridging carbons are negligible at least to the first order of approximation.[7−9] Thus, for the partial structure **E** (Figure 2), the chemical shift of the carbon marked by a dot is expected to be independent of the stereochemistry of the substituents C, D, c, and d, but dependent on the stereochemistry of the substituents A, B, a, and b.

Chart 7. Vicincal $^1H/^1H$ Spin-Coupling Constants of Triols **1a**∼**d** (Panel A), Tetraols **2a**∼**h** (Panel B), and Pentaols **3a**∼**p** (Panel C) in CD_3OD[a]

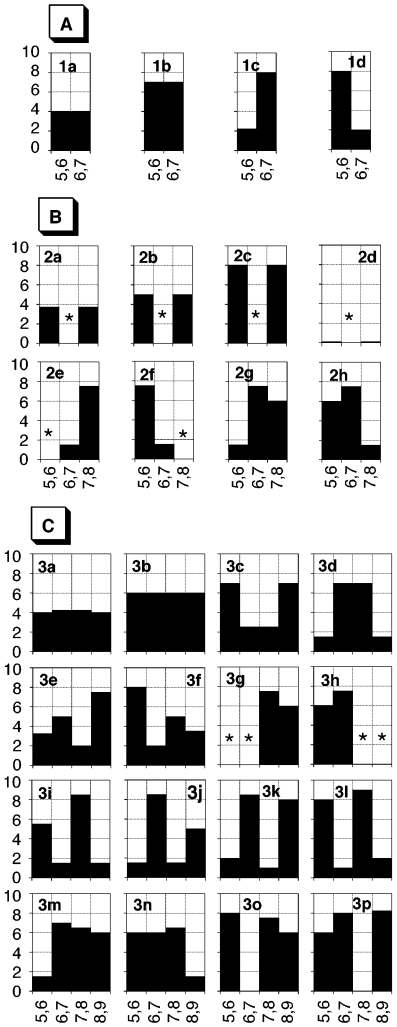

[a] The *x* and *y* axes represent proton number and the $^3J_{H,H}$ constant in Hz, respectively. The $^3J_{H,H}$'s indicated by an asterisk were not determined.

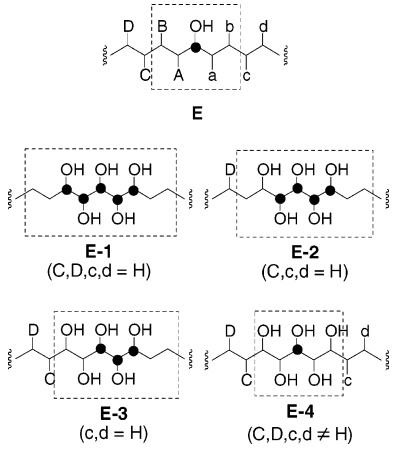

Figure 2. Self-contained boxes are highlighted by a broken line. The carbons indicated by a dot are usable for analysis.

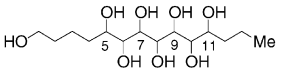

	C5	C6	C7	C8	C9	C10	C11
4a	α	α	α	α	β	α	β
4b	α	α	α	α	α	β	α
4c	β	α	β	α	β	α	β
4d	β	α	β	α	α	β	α

Figure 3. Stereochemistry of heptaols **4a**∼**d**.

Taking this characteristic into account, referred to as "self-contained nature",[7] we need to exclude certain nuclei from comparison of the NMR databases with the structural motifs present in unknown compounds. This situation is schematically exemplified with a pentaol system (Figure 2). Depending on the substitution pattern, the carbons marked with a dot are expected to be independent of the stereochemistry of the substituents present in the outside of a self-contained box and therefore can be used for comparison with NMR databases, cf., **E**−**1**, **E**−**2**, **E**−**3**, and **E**−**4**. In an extreme case such as **E**−**4**, only one carbon is available for an NMR comparison, and a conclusive stereochemical assignment might not always seem possible. However, it has been demonstrated that even for such a case, a combined use of multiple descriptors such as ^{13}C and ^{1}H chemical shifts is effective in deducing the stereochemistry of unknown compounds.[5,7,8]

We have recognized one important consequence derived from the self-contained nature of NMR databases. Because of this nature, small universal databases can be applied separately to relevant structural moieties contained in a larger stereocluster for its stereochemical analysis, and therefore, it is not required to create an NMR database to cover the entire structure of the larger stereocluster. Indeed, with only three, small NMR databases, we were able to predict correctly the relative configuration of the C21∼C38 portion of oasomycin A.[7] Adopting the same approach, we should be able to apply the contiguous polyol ^{13}C chemical shift NMR databases for stereochemical analyses of unknown higher order polyols. The NMR databases using other descriptors such as ^{1}H and ^{1}H(OH) chemical shifts can similarly be used.

To assess fully the potentials of NMR databases using different descriptors, we chose four heptaols **4a**∼**d** for a case study (Figure 3). The four heptaols **4a**∼**d** were synthesized from the synthetic intermediates used for the pentaol NMR databases. The stereochemistry of **4a**∼**d** was established in a similar manner as before, and its details are given in the Supporting Information.

The observed ^{13}C chemical shifts of **4a**∼**d** are shown in Chart 8. Each diastereomer exhibits a differing pattern from the others, thereby suggesting that the ^{13}C chemical shift profile can be utilized as a fingerprint to deduce their stereochemistry.

With the procedure outlined in Figure 2, we predicted the ^{13}C chemical shifts for the C3∼C13 carbons of **4a**∼**d**. With focus on the self-contained box indicated in the first correlation, the C3/C4/C5 chemical shifts of **4a**∼**d** were predicted, based on the **1a**∼**d** database (Figure 4). Similarly, on comparison with the **2a**∼**h** and **3a**∼**p** databases, the C4/C5/C6 and C5/C6/C7 chemical shifts of **4a**∼**d** were predicted, respectively, cf., the second and third correlations in Figure 4. Continuing this operation for the remaining carbons, we predicted the ^{13}C chemical shifts for **4a**∼**d** (Panel A, Chart 9), which were then

Chart 8. ^{13}C Chemical Shift Profile Observed for **4a**∼**d** in CD_3OD (100 MHz)[a]

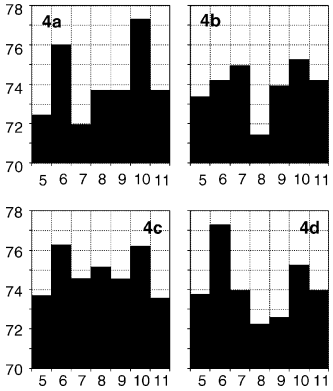

[a] The *x* and *y* axes represent carbon number and ^{13}C chemical shift in ppm, respectively.

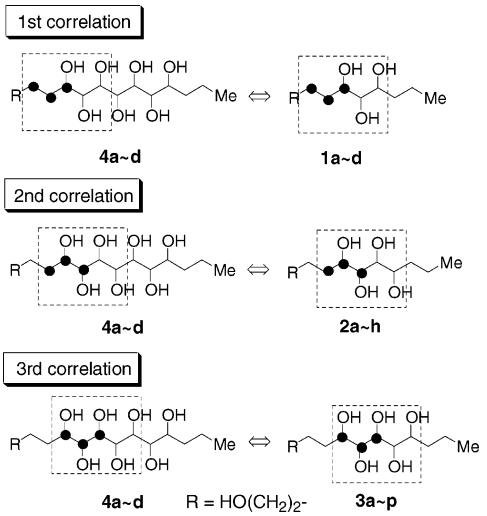

Figure 4. Protocol for predicting the ^{13}C chemical shift profile for **4a**∼**d**. Structural correlation of **4a**∼**d** with **1a**∼**d** (first correlation), **2a**∼**h** (second correlation), and **3a**∼**p** (third correlation) allows prediction of the C3/C4/C5, C4/C5/C6, and C5/C6/C7 chemical shifts of **4a**∼**d**, repectively.

compared with their observed ^{13}C chemical shifts (Panel B, Chart 9).[14,15] As seen from the comparison shown in Panel B, the ^{13}C chemical shift profiles predicted for **4c** and **4d** were found to agree well with their observed ^{13}C profiles.[16] However, the ^{13}C chemical shifts predicted for **4a** and **4b** were noticeably different from the observed profiles, thereby suggesting that the chemical shift of the self-contained carbon, cf., the carbon marked by a dot in **E** (Figure 2), is affected even by a functional group(s) present in the outside of a self-contained box. Clearly, it is desirable to formulate an increment(s) to count in these

(14) The C3∼C5 and C11∼C13 stereoclusters present in **4a**∼**d** can be represented by the C3∼C5 and C7∼C9 moieties in the triol series, the C3∼C5 and C8∼10 in the tetraol series, or the C3∼C5 and C9∼C11 moieties in the pentaol series. In this prediction, the profiles observed for **1a**∼**d** were used to estimate the C3∼5 and C11∼13 chemical shifts of **4a**∼**d**. Similarly, the profiles of **2a**∼**h** were used to estimate the C6 and C10 chemical shifts of **4a**∼**d**. The profiles observed for **3a**∼**p** were used to estimate the remaining ^{13}C chemical shifts of **4a**∼**d**. For the detailed procedure, see the Supporting Information.

(15) Charts 9∼13 show the profiles covering the C5∼C11 portions only. The complete profiles are included in Supporting Information.

(16) In the NMR database approach, a match/mismatch judgment is made, on the basis of an overall fitness of the *predicted profile*, rather than a single data point, over the *observed profile*. Nevertheless, from a large number of examples studied in this laboratory, we consider the 0.5 and 0.03 ppm differences in ^{13}C and ^{1}H chemical shifts, respectively, to be significant even for a comparison of a single data point.

Chart 9. Panel A: ^{13}C Chemical Shift Profiles Predicted for **4a**∼**d** and Panel B: Difference between the Observed and Predicted ^{13}C Chemical Shift Profiles (100 MHz, CD_3OD)[a]

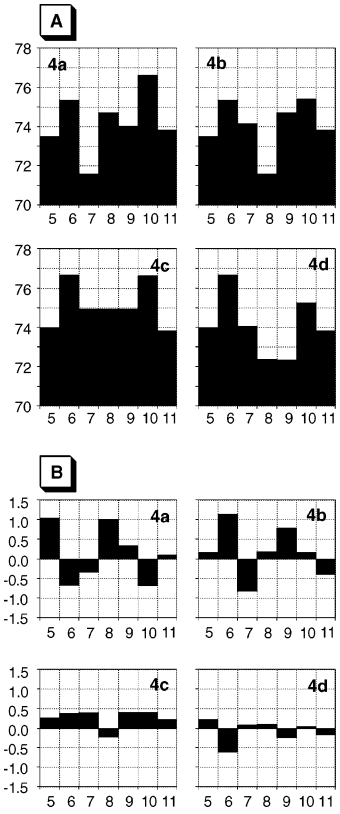

[a] The *x* axis represents carbon number and the *y* axis represents ^{13}C chemical shift (Panel A) and $\Delta\delta = \delta_{predicted} - \delta_{observed}$ (Panel B) in ppm.

effects on the NMR databases. Thus, we have conducted the following comparisons.

Assuming no effect from a functional group present in the outside of the self-contained box indicated, we would expect an identical or at least a close chemical shift for the C3, C4, and C5 carbons of **1a** in the triol series, **2a**,**e** in the tetraol series, and possibly **3a**,**e**,**g**,**i** in the pentaol-series,[17] because the 1,2,3-triol system present in these substrates bears the same stereochemistry. The same stereochemical environment is shared by the substrates belonging to the sub-groups of **1b**/**2h,b**/**3h**,**p**,**b**,**n**, **1c**/**2g**,**d**/**3d**,**m**,**k**,**j**, and **1d**/**2c**,**f**/**3l**,**o**,**c**,**f**, respectively. Thus, through the comparison of the C3, C4, and C5 chemical shifts observed for **1a**∼**d** with those observed for the corresponding sub-group members of **2a**∼**h** and **3a**∼**p**, it is possible to estimate the effects on the chemical shift from the functional group(s) present in the outside of self-contained boxes (Panel A, Figure 5 and Table 1).

This exercise sheds light on several characteristics of a self-contained box. First, the C3 chemical shift observed for all the substrates is clustered within the 0.1-ppm range, suggesting that the stereochemical information is not transmitted from the C8 hydroxyl group to the C3 carbon in a significant degree, and therefore, it is not necessary to take this effect into account for refinement of the predicted profiles. Second, the C5 chemical

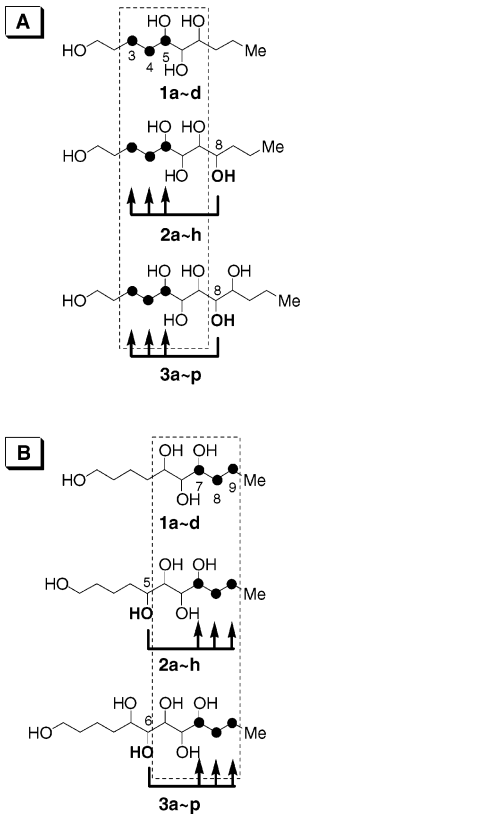

Figure 5. Estimation of the effect on ^{13}C chemical shift from the hydroxyl group(s) present in the outside of the self-contained box indicated by a broken line. Panel A: A comparison of the C3/C4/C5 chemical shifts of **1a**∼**d** with those of **2a**∼**h** and **3a**∼**p** allows estimation of the degree of effect from the C8 hydroxyl group over the C3/C4/C5 ^{13}C chemical shifts. Panel B: A comparison of the C7/C8/C9 chemical shifts of **1a**∼**d** with the C8/C9/C10 of **2a**∼**h** and the C9/C10/C11 of the **3a**∼**p** allows estimation of the degree of effect from the C5 (**2a**∼**h**) or C6 (**3a**∼**p**) over the C7/C8/C9 ^{13}C chemical shifts.

shifts observed spread over the range of $+1.2 \sim -1.0$ ppm, demonstrating that the self-contained carbons are affected even by the hydroxyl group(s) present in the outside of a self-contained box. Interestingly, the chemical shifts observed for the substrates belonging to the **1b**/**2h,b**/**3h**,**p**,**b**,**n**, **1c**/**2g**,**d**/**3d**,**m**,**k**,**j**, and **1d**/**2c**,**f**/**3l**,**o**,**c**,**f**, sub-groups are clustered within the 0.5-ppm range,[16] whereas only those for the substrates belonging to the **1a**/**2a,e**/**3a**,**e**,**g**,**i** sub-group spread over a wide range. In other words, the magnitudes of this effect depend on a specific stereochemical arrangement of the hydroxyl groups present in not only the outside but also the inside of a self-contained box. Therefore, on application of the concept of self-contained box to stereochemical analysis, a small increment due to this effect, referred to as a γ-effect,[18] needs to be added to refine the profile predicted for some stereoisomers at the first-order approximation. Third, the C4 chemical shifts spread over the range of $+0.3 \sim -0.7$ ppm. Once again, the degree of deviation depends on a specific stereochemical arrangement of

(17) Strictly speaking, the effect from the C9−OH is included in the triol/pentaol-comparison. To estimate the γ- and δ-effects further, we have also conducted the comparison of the C4/C5/C6-chemical shifts observed in the tetraol series over the pentaol and found the overall trend of this comparison to be similar to the one discussed in the text.

(18) The γ- and δ-effects are referred to the effects by a substituent on the carbon connected to the nuclei in question with two- and three-bridging carbons, respectively. The $\Delta\delta$'s at C4 and C5 obtained from the triol/tetraol-comparison represent the γ- and δ-effects from the C8−OH, respectively (Table 1). On the other hand, the $\Delta\delta$'s at C4 and C5 obtained from the triol/pentaol-comparison include the δ- and γ-effects from the C8−OH as well as the ϵ- and δ-effects from the C9−OH. Likewise, the $\Delta\delta$'s at H5 include the δ-effect from the C8−OH in the triol/tetraol-comparison and the δ- and ϵ-effects from the C8− and C9−OH's in the triol/pentaol-comparison (Table 2).

Table 1. Comparison between ^{13}C Chemical Shifts at C3, C4, and C5 of Triols **1a**∼**d** and Those of Tetraols **2a**∼**h** and Pentaols **3a**∼**p**[a]

	Relative Configuration C5 C6 C7 C8 C9	Chemical Shift (δ) C3	C4	C5	Δδ = δ(**2** or **3**) - δ(**1**) C3	C4	C5
1a	α α α	23.12	34.51	73.51	Δδ = δ(**2** or **3**) - δ(**1a**)		
2a	α α α α	23.21	34.26	72.97	+0.1	-0.3	-0.5
3a	α α α α α	23.15	34.32	73.01	+0.0	-0.2	-0.5
3e	α α α α β	23.24	34.41	72.49	+0.1	-0.1	-1.0
2e	α α α β	23.03	34.05	74.49	-0.1	-0.5	+1.0
3g	α α α β α	23.02	34.05	74.45	-0.1	-0.5	+1.0
3i	α α α β β	23.04	34.11	74.68	-0.1	-0.4	+1.2
1b	α β α	22.96	33.25	73.98	Δδ = δ(**2** or **3**) - δ(**1b**)		
2h	α β α α	22.99	32.75	74.21	0.0	-0.5	+0.2
3h	α β α α α	22.99	32.77	74.28	0.0	-0.5	+0.3
3p	α β α α β	22.99	32.74	74.21	0.0	-0.5	+0.2
2b	α β α β	23.05	32.60	73.95	+0.1	-0.7	0.0
3b	α β α β α	23.01	33.16	73.53	+0.1	-0.1	-0.5
3n	α β α β β	23.08	32.96	73.96	+0.1	-0.3	0.0
1c	α α β	23.34	34.58	71.50	Δδ = δ(**2** or **3**) - δ(**1c**)		
2g	α α β α	23.38	34.49	71.71	0.0	-0.1	+0.2
3d	α α β α α	23.36	34.48	71.73	0.0	-0.1	+0.2
3m	α α β α β	23.36	34.45	71.81	0.0	-0.1	+0.3
2d	α α β β	23.46	34.55	71.54	+0.1	0.0	0.0
3k	α α β β α	23.46	34.56	71.40	+0.1	0.0	-0.1
3j	α α β β β	23.44	34.58	71.08	+0.1	0.0	-0.4
1d	α β β	22.99	34.46	72.73	Δδ = δ(**2** or **3**) - δ(**1d**)		
2c	α β β α	23.05	34.55	72.88	+0.1	+0.1	+0.2
3l	α β β α α	23.05	34.75	73.02	+0.1	+0.3	+0.3
3o	α β β α β	23.01	34.66	72.64	0.0	+0.2	-0.1
2f	α β β β	22.96	34.26	72.51	0.0	-0.2	-0.2
3c	α β β β α	22.99	33.92	72.56	0.0	-0.5	-0.2
3f	α β β β β	22.97	34.34	72.61	0.0	-0.1	-0.1

[a] δ and Δδ = δ(tetraol or pentaol) − δ(triol) are in ppm. A box highlights the same relative stereochemistry shared with all the members in each sub-group.

the hydroxyl groups present in both the outside and inside of a self-contained box. As expected, the magnitude of this effect, referred to as a δ-effect,[18] is less significant than that of the γ-effect. Nevertheless, to refine the profile predicted at the first order of approximation, we suggest including an increment due to δ-effects as well.

With focus on the C7, C8, and C9 carbons, a similar comparison of the triol series over the tetraol series, as well as the pentaol series, was made (Panel B, Figure 5).[19] An overall trend found in the C7/C8/C9-comparison was found to be virtually identical to the trend found in the C3/C4/C5-carbon comparison. Once again, the C7 chemical shifts of **1a**∼**d**, corresponding to the C5 chemical shifts in the first comparison, in three out of four sub-groups were found to be clustered within the range of 0.4 ppm, whereas those in the forth sub-group were found to spread over the range of +1.2 ∼ −1.0 ppm. The behaviors of the C8 and C9 chemical shifts were well compared with those to the C4 and C3 chemical shifts in the previous comparison, respectively. Interestingly, the substrates sharing the same stereochemical arrangement of hydroxyl groups were found to exhibit almost identical behavior in the two series of comparison. These observations support the previous statement, i.e., the magnitudes of γ- and δ-effects depend on a specific stereochemical arrangement of the hydroxyl groups present in both the inside and outside of self-contained boxes.

(19) For the details, see the Supporting Information.

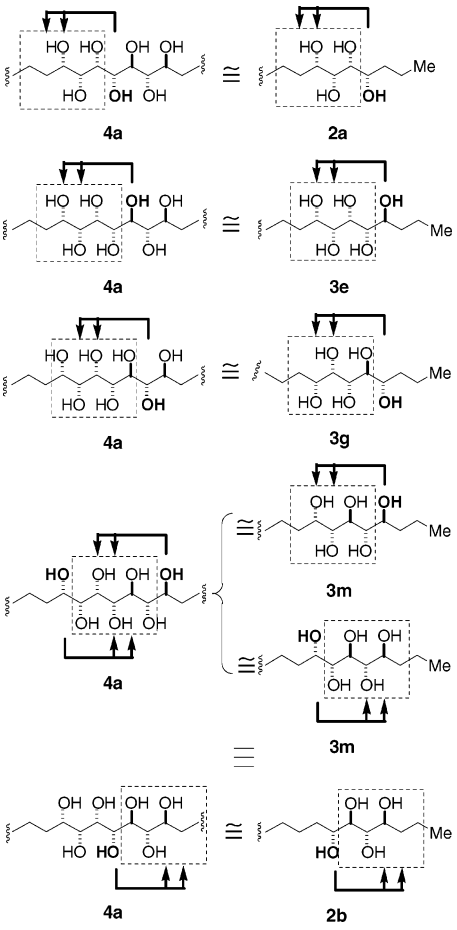

Figure 6. Procedure used for refining the ^{13}C chemical shift profile predicted for **4a** by addition of the estimated γ- and δ-effects of the hydroxyl groups present in the outside of the self-contained box.

Back to the predicted and experimental ^{13}C chemical shifts of **4a**∼**d**, it is interesting to note that the identified, specific stereochemical arrangement is incorporated in the stereochemical array of **4a** and **4b**, but is not in the stereochemical array of **4c** and **4d**. With use of the γ- and δ-effects listed in Table 1, the predicted ^{13}C profiles were refined for **4a**∼**d** in the stepwise manner as exemplified for **4a** in Figure 6. The γ- and δ-effects of the C8−OH group on the C5 and C4 carbons of **4a** were approximated with those found in the comparison of **1a** with **2a**. Similarly, the γ- and δ-effects of the C9−OH group on the C6 and C5 carbons were approximated with those found in the comparison of **2a** with **3e**, and so on. The refined, predicted ^{13}C profiles thus obtained, including those of **4a** and **4b**, match well with their observed ^{13}C chemical profiles (Chart 10).

Overall, an analysis only with a self-contained box predicts an NMR profile satisfactorily similar to the observed profile for some stereoisomers, but significantly different from the observed profile for others. The discrepancy between the predicted and observed profile is primarily due to γ- and δ-effects. Importantly, the magnitudes of γ- and δ-effects depend on a stereochemical arrangement of the functional groups present in both the inside and outside of a self-contained box.

Chart 10. Panel A: Refined, Predicted ^{13}C Chemical Shift Profiles of **4a**∼**d** and Panel B: Difference between the Observed and Refined, Predicted ^{13}C Chemical Shift Profiles (100 MHz, CD_3OD)[a]

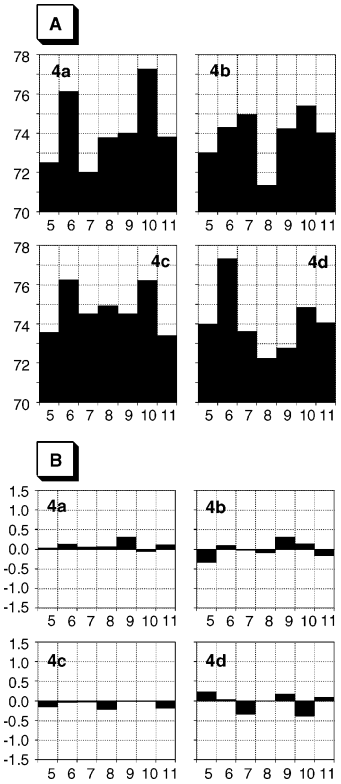

[a] The *x* axis represents carbon number and the *y* axis represents ^{13}C chemical shift (Panel A) and $\Delta\delta = \delta_{predicted} - \delta_{observed}$ (Panel B) in ppm.

Except the stereochemical arrangement of functional groups belonging to a specific sub-group, the γ- and δ-effects can, at least at the first order of approximation, be ignored for the stereochemical analysis of unknown compounds. However, for the stereoisomers belonging to the specific sub-group, it is necessary to refine the profile predicted at the first order of approximation, with incorporation of the γ- and δ-effects. With these procedures, it is possible to properly predict an NMR profile for unknown polyols. However, as discussed later, an analytical procedure using a $^3J_{H,H}$ profile is *operationally simpler* than this procedure. Therefore, we suggest a $^3J_{H,H}$ profile as the primary device for predicting the stereochemistry of unknown polyols and a ^{13}C chemical shift profile as the secondary device to confirm the predicted stereochemistry.

It is worth adding that the γ- and δ-effects are also noticed on some stereoclusters related to the polyketide class of natural products. Once again, the magnitudes of γ- and δ-effects have been found to depend on a specific stereochemical arrangement of the functional groups present in both the inside and outside of a self-contained box. A significant magnitude of these effects has been observed only for the stereoisomers belonging to a specific sub-group and, interestingly, this specific sub-group shares the same stereochemical array with the sub-group in the contiguous polyol series.[20]

b. Proton Chemical Shift NMR Database. Similarly as the ^{13}C chemical shift databases, the ^1H chemical shift NMR databases created for the 1,2,3-triol, 1,2,3,4-tetraol, and 1,2,3,4,5-pentaol systems can be used for stereochemical analysis of unknown compounds bearing these structural motifs. It is worth noting that the ^{13}C and ^1H chemical shift databases often provide complementary information each other[5,7,8] and therefore, whenever possible, we suggest a combined use of both databases for stereochemical analysis of unknown compounds.

To illustrate this point, **4a**∼**d** are again used for a case study. The observed ^1H chemical shifts of **4a**∼**d** are shown in Chart 11. Each diastereomer exhibits a differing profile from the others, thereby indicating that the ^1H chemical shift profile can be used as a tool to deduce its stereochemistry.

With the procedure depicted in Figure 4, the ^1H chemical shift profile was predicted for **4a**∼**d** without consideration of the effects from the outside of a self-contained box (Panel A, Chart 12), and the differences between the predicted and observed profiles are shown (Panel B, Chart 12). For all of **4a**∼**d**, significant differences are noticed between the predicted and observed profiles, thereby raising a question on the

Chart 11. ^1H Chemical Shift Profiles Observed for **4a**∼**d** in CD_3OD (500 MHz)[a]

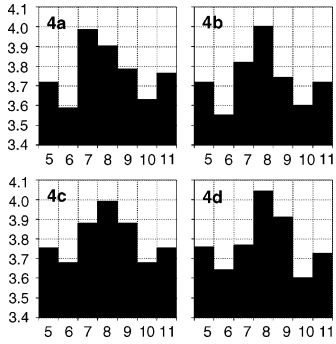

[a] The *x* and *y* axes represent proton numbers and ^1H chemical shift in ppm.

Chart 12. Panel A: ^1H Chemical Shift Profiles Predicted for **4a**∼**d** and Panel B: Difference between the Observed and Predicted ^1H Chemical Shift Profiles (500 MHz, CD_3OD)[a]

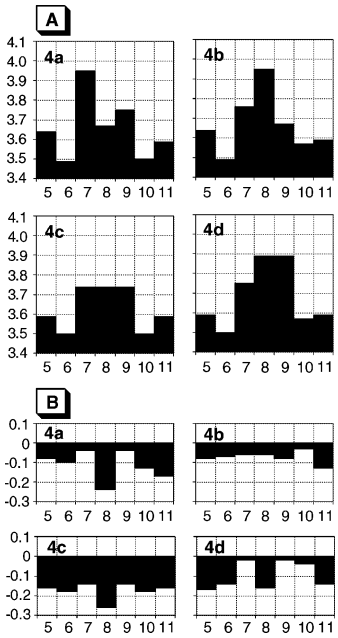

[a] The *x* axis represents proton number and the *y* axis represents ^1H chemical shift (Panel A) and $\Delta\delta = \delta_{predicted} - \delta_{observed}$ (Panel B) in ppm.

(20) Zeng, H.; Kishi, Y. unpublished work.

Table 2. Comparison between ^{1}H Chemical Shifts at H5 of Triols **1a**∼**d** and Those of Tetraols **2a**∼**h** and Pentaols **3a**∼**p**[a]

	Relative Configuration C5 C6 C7 C8 C9	Chemical Shift (δ) H5	Δδ = δ(**2** or **3**) - δ(**1**) H5
1a	α α α	3.64	Δδ = δ(**2** or **3**) - δ(**1a**)
2a	α α α α	3.70	+0.06
3a	α α α α α	3.72	+0.08
3e	α α α α β	3.70	+0.06
2e	α α α β	3.66	+0.02
3g	α α α β α	3.68	+0.04
3i	α α α β β	3.70	+0.06
1b	α β α	3.59	Δδ = δ(**2** or **3**) - δ(**1b**)
2h	α β α α	3.70	+0.11
3h	α β α α α	3.70	+0.11
3p	α β α α β	3.71	+0.12
2b	α β α β	3.73	+0.14
3b	α β α β α	3.74	+0.15
3n	α β α β β	3.76	+0.17
1c	α α β	3.81	Δδ = δ(**2** or **3**) - δ(**1c**)
2g	α α β α	3.83	+0.02
3d	α α β α α	3.87	+0.06
3m	α α β α β	3.86	+0.05
2d	α α β β	3.83	+0.02
3k	α α β β α	3.84	+0.03
3j	α α β β β	3.83	+0.02
1d	α β β	3.59	Δδ = δ(**2** or **3**) - δ(**1d**)
2c	α β β α	3.62	+0.03
3l	α β β α α	3.64	+0.05
3o	α β β α β	3.63	+0.04
2f	α β β β	3.62	+0.03
3c	α β β β α	3.64	+0.05
3f	α β β β β	3.64	+0.05

[a] δ and $\Delta\delta = \delta$(tetraol or pentaol) − δ(triol) are in ppm. A box highlights the same relative stereochemistry shared with all the members in each sub-group.

predictability of ^{1}H chemical shift profiles. It is interesting to note that all these discrepancies are observed in a negative direction, i.e., all the predicted ^{1}H chemical shifts are in more upfields than the observed values.

We were curious in estimating the effects from the hydroxyl groups present in the outside of a self-contained box. It should be noted that, because of one extra nucleus present between the two functional groups concerned, the self-contained box already includes the γ-effect in the ^{1}H chemical shift profiles.[18] With application of the procedure outlined in Figure 6, the H5 chemical shifts of **1a**∼**d** were compared with those of **2a**∼**h** and **3a**∼**p**, yielding an approximate δ-effect (Table 2).[17] As seen in the ^{13}C chemical shifts, the magnitudes of δ-effects depend on a specific stereochemical arrangement of the hydroxyl groups present in both the outside and inside of a self-contained box. Interestingly, parallel with the ^{13}C series, the members in the **1b** sub-group exhibit the most significant deviation.

With use of the estimated δ-effects listed in Table 2, the ^{1}H chemical shift profiles predicted for **4a**∼**d** were refined, thereby yielding the profiles matching well with the observed profiles (Chart 13).

Overall, an analysis at the first order of approximation, i.e., with focus only on a self-contained box, does not give the ^{1}H chemical shift profiles satisfactorily for stereochemical analysis of unknown polyols. However, an analysis with the δ-effects included yields a good match between the ^{1}H chemical shift profiles and the observed profiles, thereby demonstrating the value of ^{1}H chemical shift profiles for stereochemical analysis of unknown polyols. However, as mentioned before, an analytical procedure using a $^3J_{H,H}$ profile is *operationally simpler* than this procedure. Therefore, we suggest a $^3J_{H,H}$ profile as the primary device for predicting the stereochemistry of unknown higher polyols and a ^{1}H chemical shift profile as the secondary device to confirm the predicted stereochemistry.

Chart 13. Panel A: Refined, Predicted ^{1}H Chemical Shift Profiles of **4a**∼**d** and Panel B: Difference between the Observed and Refined, Predicted ^{1}H Chemical Shift Profiles[a]

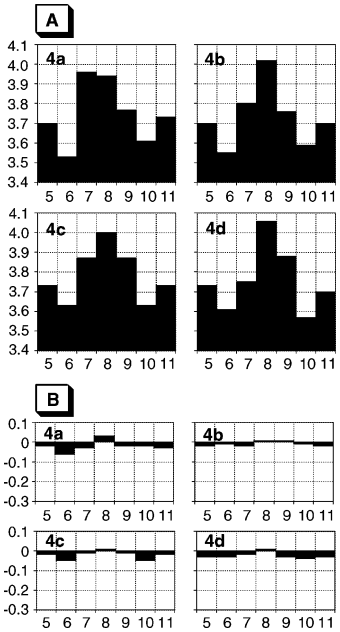

[a] The *x* axis represents proton number and the *y* axis represents ^{1}H chemical shift (Panel A) and $\Delta\delta = \delta_{predicted} - \delta_{observed}$ (Panel B) in ppm.

c. Vicinal ^{1}H/^{1}H Spin-Coupling NMR Database. With a 1,2-disubstituted system, it is known as a general trend that a *syn*-diol gives a smaller $^3J_{H,H}$ constant than the corresponding *anti*-diol. The $^3J_{H,H}$'s observed for pentaols **3a**∼**p** are organized under two sub-groups, (1) $^3J_{6,7}$ and $^3J_{7,8}$ constants, referred to as the internal $^3J_{H,H}$'s (Panel A, Chart 14), and (2) $^3J_{5,6}$ and $^3J_{8,9}$ constants, referred to as the terminal $^3J_{H,H}$'s (Panel A, Chart 15). As seen from these Charts, the general trend, i.e., a *syn*-diol gives a smaller $^3J_{H,H}$ constant than the corresponding *anti*-diol, is recognized for both the internal and terminal $^3J_{H,H}$ constants. However, the $^3J_{H,H}$ constants observed for these substrates spread in a wide range and, critically, the $^3J_{H,H}$ constants observed for some of *syn*-diols in both of internal and terminal series are very close to those for *anti*-diols. Because of this fact, it is not a straightforward task to translate a single $^3J_{H,H}$ constant to a *syn*- or *anti*-stereochemistry present in an unknown compound.[21] Remarkably, 17 out of the 24 $^3J_{H,H}$

(21) To overcome this difficulty, Murata and co-workers have suggested a combined use of $^3J_{H,H}$, $^3J_{H,C}$, and $^2J_{H,C}$ constants and NOE and this approach has been applied to predict the stereochemistry of several unknown natural products: Matsumori, N.; Kaneno, D.; Murata, M.; Nakamura, H.; Tachibana, K. *J. Org. Chem.* **1999**, *64*, 866−876. For reviews of this approach, see: Murata, M.; Yasumoto, T. *Nat. Prod. Rep.* **2000**, *17*, 293−314; Riccio, R.; Bifulco, G.; Cimino, P.; Bassarello, C.; Gomez-Paloma, L. *Pure. Appl. Chem.* **2003**, *75*, 295−308.

Chart 14. Panel A: Internal $^3J_{H,H}$'s of Pentaols **3a**∼**p**; Panel B: Sub-grouped, Internal $^3J_{H,H}$'s[a]

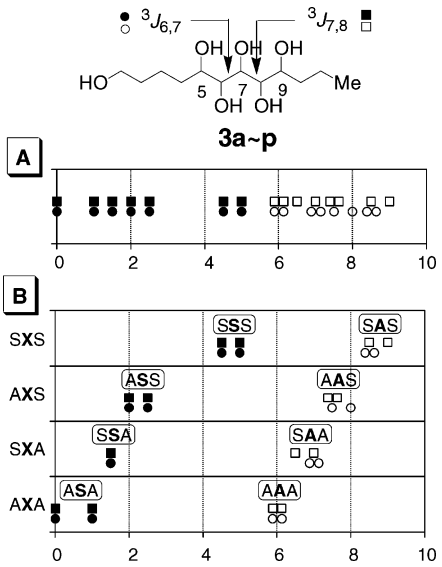

[a] The *y* axis indicates the stereochemistry of the adjacent glycols, representing A = *anti*, S = *syn*, and X = stereochemistry at 6/7 or 7/8. The *x* axis gives the $^3J_{H,H}$'s observed for the 6,7- and 7,8-glycol systems, with ● and ○ representing the *syn*- and *anti*-6,7-glycols, respectively, whereas with ■ and □ representing the *syn*- and *anti*-7,8-glycols.

Chart 15. Panel A: Terminal $^3J_{H,H}$'s of Pentaols **3a**∼**p**; Panel B: Sub-grouped, Terminal $^3J_{H,H}$'s, Including the Stereochemistry of the Adjacent Glycol Only; Panel C: Sub-grouped, Terminal $^3J_{H,H}$'s, Including the Stereochemistry of the Adjacent and Next Glycols[a]

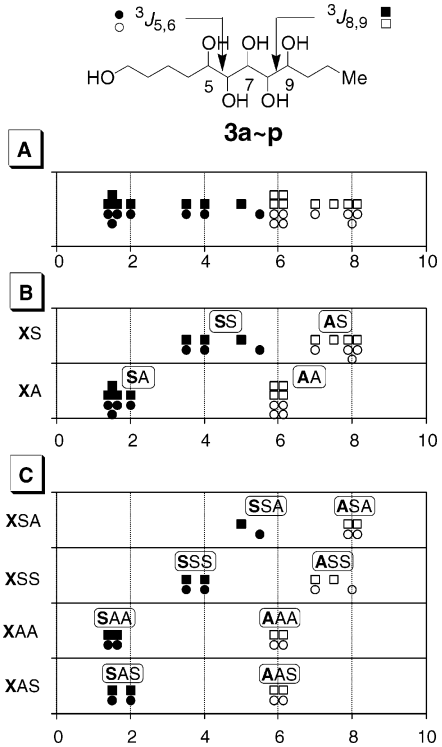

[a] The *x* axis gives the $^3J_{H,H}$'s observed for the 5,6- and 8,9-glycol systems, with ● and ○ representing the *syn*- and *anti*-5,6-glycols, respectively, whereas with ■ and □ representing the *syn*- and *anti*-8,9-glycols. The *y* axis indicates the stereochemistry of the adjacent glycols, representing A = *anti*, S = *syn*, and X = stereochemistry at 5/6 or 8/9.

constants observed for **4a**∼**d** were in the border-line (6 ± 1 Hz) region (Table 3).

Table 3. $^3J_{H,H}$'s Observed on Heptaols **4a**∼**d** in Hz (500 MHz, CD_3OD)

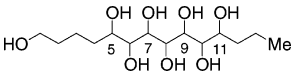

	5/6	6/7	7/8	8/9	9/10	10/11
4a	3.5	5.0	2.0	7.0	6.0	6.0
4b	3.5	4.0	5.0	1.5	7.5	6.0
4c	6.5	6.0	6.0	6.0	6.0	6.5
4d	6.0	6.0	6.0	0.0	7.0	6.0

One of the key logics used for developing the NMR database approach was to analyze a *profile*, rather than a single datapoint, to deduce the stereochemistry of an unknown compound. The following simple exercise immediately indicates that this logic is powerful also for analyzing the characteristics of $^3J_{H,H}$ constants. Depending on the relative stereochemistry of the adjacent glycols, the internal *syn*, abbreviated as S, and *anti*, abbreviated as A, diols are divided into the S**X**S, A**X**S, S**X**A, and A**X**A sub-groups, respectively, and their $^3J_{H,H}$ constants were analyzed. As seen from Panel B in Chart 14, the $^3J_{H,H}$ constants observed for S**S**S, A**S**S, S**S**A, A**S**A, S**A**S, A**A**S, S**A**A, and A**A**A sub-groups now cluster in a much narrower range.

Similarly, we tested the terminal *syn*- and *anti*-diols. For the first attempt, we used only the adjacent internal glycol to divide the terminal *syn*- and *anti*-diols into the **X**S and **X**A sub-groups. As seen from Panel B in Chart 15, the $^3J_{H,H}$ constants in the **S**A, **A**A, and **A**S sub-groups cluster in a narrower range, but those in the **S**S sub-group still spread in a wide range. Interestingly, including the relative stereochemistry of the glycol system one further away, i.e., dividing them into the **X**SA, **X**SS, **X**AA, and **X**AS sub-groups, the $^3J_{H,H}$ constants in all the sub-groups now cluster in a much narrower range (Panel C, Chart 15). This result is not surprising; namely, with an additional parameter included, a higher resolution should be obtained on the NMR profiles.[22]

The sub-grouping exercise convincingly indicates the potentials that the $^3J_{H,H}$-based NMR profiles offer for stereochemical analysis of unknown compounds. We first examined the $^3J_{H,H}$ profiles composed of the two adjacent spin-coupling constants. These profiles are described by placing the first and second $^3J_{H,H}$'s on the X- and Y-axes, respectively. Panels A and B in Chart 16 show the profiles thus obtained for the internal and terminal $^3J_{H,H}$ pairs present in **3a**∼**p**. Depending on their relative stereochemistry, the internal $^3J_{H,H}$ pairs are distributed in four areas, cf., S/A, S/S, A/A, and A/S. For the case of terminal $^3J_{H,H}$ pairs, the S/A, A/A, and A/S pairs are distributed in relatively narrow areas, whereas the S/S pairs are spread over a wider area. However, including the glycol system of one further away for analysis, i.e., dividing the S/S-group into the S/S/S- and S/S/A-sub-groups, the $^3J_{H,H}$ pairs now cluster in narrow areas.

The $^3J_{H,H}$ profiles thus obtained for the internal and terminal pairs of $^3J_{H,H}$ constants are useful for analyzing the relative

(22) On comparison with the $^3J_{H,H}$ distributions shown in Charts 10B and 11C, it is possible to analyze the relative stereochemistry of unknown contiguous polyols. In this approach, the stereochemical analysis is conducted, one at a time, based on one vicinal spin-coupling constant as a function of the relative stereochemistry of the adjacent glycols. However, in the terms of applicability and ease-of-use, we assess the analytical procedures discussed in the text to be far superior to this procedure. The details of procedure are given for **4a**∼**d** in the Supporting Information.

Chart 16. 2D-Representation of the Internal (Panel A) and Terminal (Panel B) $^3J_{H,H}$'s Observed for Triols **3a**∼**p**[a]

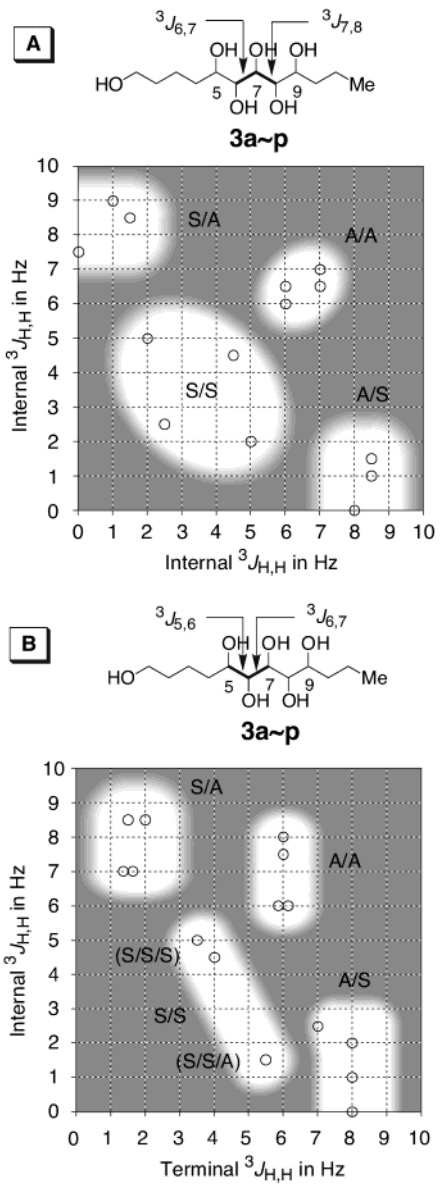

[a] The *x* and *y* axes represent the two contiguous $^3J_{H,H}$'s indicated by arrows on 3a∼p, with abbreviations of S = *syn* and A = *anti*.

stereochemistry of unknown compounds. For example, on comparison with these profiles, the observed $^3J_{5,6}$ = 3.5 (terminal), $^3J_{6,7}$ = 5.0 (internal), $^3J_{7,8}$ = 2.0 (internal), $^3J_{8,9}$ = 7.0 (internal), $^3J_{9,10}$ = 6.0 (internal), and $^3J_{10,11}$ = 6.0 (terminal) correctly predict the relative stereochemistry of **4a** at C5/C6/C7, C6/C7/C8, C7/C8/C9, C8/C9/C10, C9/C10/C11, C10/C11/C12 to be S/S, S/S, S/A, A/A, A/A, respectively, cf., the filled circles marked in Panels A and B in Chart 17. Similarly, the relative stereochemistry of **4b**∼**d** can be correctly predicted as included in Supporting Information.

The $^3J_{H,H}$ profiles discussed above are composed of the two adjacent vicinal spin-coupling constants. Naturally, we were interested in the stereochemical analysis with the three contiguous vicinal spin-coupling constants; with an addition of the third vicinal spin-coupling constant, we would expect a higher resolution on the NMR profile and the resultant NMR profile to become a more powerful device for stereochemical analysis.

Chart 17. Prediction of the Relative Stereochemistry of **4a**, by Plotting the Observed, Two Contiguous $^3J_{H,H}$'s on the Internal (Panel A) and Terminal (Panel B) 2D-panels[a]

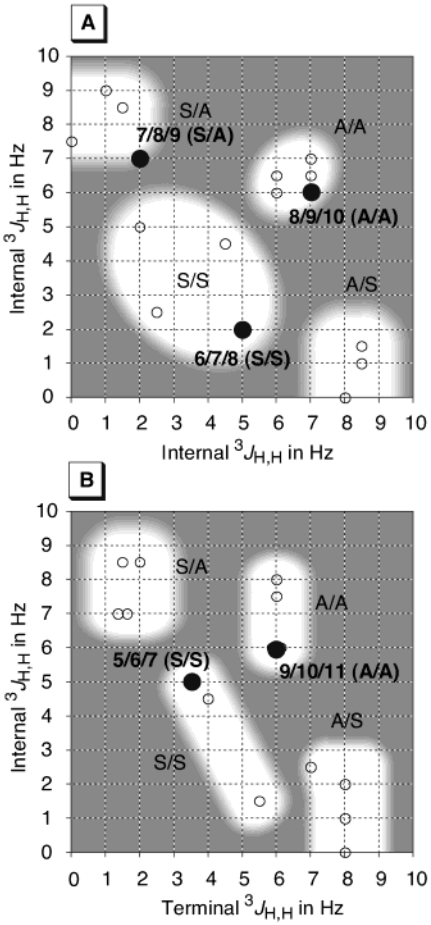

[a] The *x* and *y* axes represent $^3J_{H,H}$'s, with abbreviations of A = *anti*, S = *syn*. The filled circle gives the two contiguous $^3J_{H,H}$'s observed on 4a, with indications of the position and stereochemistry; for example, 5/6/7 (S/S) represents $^3J_{5,6}/^3J_{6,7}$ (the relative configuration at 5/6 and 6/7 = *syn* and *syn*).

The $^3J_{H,H}$ profiles composed of three contiguous spin-coupling constants could be given in a 3D presentation by placing the first, second, and third $^3J_{H,H}$ constants on the *X*-, *Y*-, and *Z*-axes, respectively. However, for convenience of the presentation, we chose to depict the profiles composed of three contiguous $^3J_{H,H}$ constants in a 1D format.

Using all the relevant spin-coupling constants observed on **3a**∼**p**, the profiles composed of three contiguous $^3J_{H,H}$ constants in CD_3OD were created (Chart 18). There are several comments worthy to make. First, practically identical $^3J_{H,H}$ profiles were observed in pyridine-d_6, DMSO-d_6, and D_2O. Second, a virtually identical $^3J_{H,H}$ profile is recognized for all the members belonging to each of the AAA, SAS, AAS, SAA, and ASA sub-groups, regardless of whether they are at the internal or terminal position. Third, two different $^3J_{H,H}$ profiles are recognized for the SSS, SSA, and ASS sub-group members, depending on the glycol system at one remote position, cf., the profiles of the SSS(S) vs SSS(A) sub-groups as well as (A)-SSA vs (S)SSA and ASS(A) vs ASS(S). Forth, the AAA and SSS(S) sub-groups seem to exhibit a similar overall profile. However, it should be noted that $^3J_{H,H}$ constants for the AAA sub-group members are around 6 Hz, whereas those for the SSS-

Chart 18. $^3J_{H,H}$ Profiles Composed of Three Contiguous Spin-Coupling Constants[a]

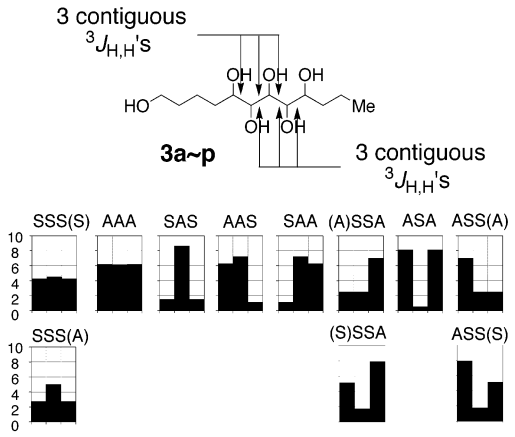

[a] The *y* axis represents $^3J_{H,H}$'s, with abbreviations of A = *anti* and S = *syn*.

(S) sub-group members are around 4 Hz. The 2 Hz difference in $^3J_{H,H}$ constants is significant in this analysis. Fifth, similarly, the overall profile of the (S)SSA and ASS(S) sub-group members may seem to be similar to that of the ASA sub-group members, but the differences in $^3J_{H,H}$ constants between them are significantly large. Sixth, tetraols **2a**~**h** contain the three contiguous $^3J_{H,H}$ systems and are expected to exhibit the profiles corresponding to those defined in the pentaol series. Indeed, **2a**~**h** give the expected profiles, cf., Panel B, Chart 7.

Overall, the profile recognized for each sub-group member is distinct and different from others. Naturally, these NMR profiles can be refined further by incorporating additional spin-coupling constants for analysis. However, as it will be seen from the case of **4a**~**d**, the NMR profiles composed of only the three contiguous spin-coupling constants are, at least to the first order of analysis, sufficient for stereochemical analysis of unknown contiguous polyols.

For the analysis using the profiles composed of three contiguous $^3J_{H,H}$ constants, an unknown compound is *imaginarily* dissected into small stereoclusters composed of three contiguous $^3J_{H,H}$ systems and the resultant $^3J_{H,H}$ profile of each small stereocluster is compared with the $^3J_{H,H}$ profiles shown in Chart 18. With **4a** as an example, this analytical procedure is outlined in Chart 19. The $^3J_{H,H}$ constants observed for **4a** are imaginarily dissected into the profiles composed of three contiguous constants, i.e., $^3J_{5,6}/^3J_{6,7}/^3J_{7,8}$ (first profile), $^3J_{6,7}/^3J_{7,8}/^3J_{8,9}$ (second profile), $^3J_{7,8}/^3J_{8,9}/^3J_{9,10}$ (third profile), and $^3J_{8,9}/^3J_{9,10}/^3J_{10,11}$ (fourth profile) and each of the profiles is compared with the profiles shown in Chart 18. This comparison allows us to immediately predict the relative stereochemistry at C5/C6/C7/C8, C6/C7/C8/C9, C7/C8/C9/C10, and C8/C9/C10/C11 to be SSS(A), (S)SSA, SAA, and AAA, respectively and, therefore, the relative stereochemistry of **4a** at C5/C6/C7/C8/C9/C10/C11 is SSSAAA. With the application of the same analytical procedure, the relative stereochemistry of **4b**~**d** is correctly predicted. The details of this analysis are given in the Supporting Information.

Vicinal spin coupling constants were reported for the polyols derived from hexoses and heptoses in the literature.[23] With the reported constants, we have created their $^3J_{H,H}$ profiles and

Chart 19. Comparison of the $^3J_{H,H}$ Profiles[a]

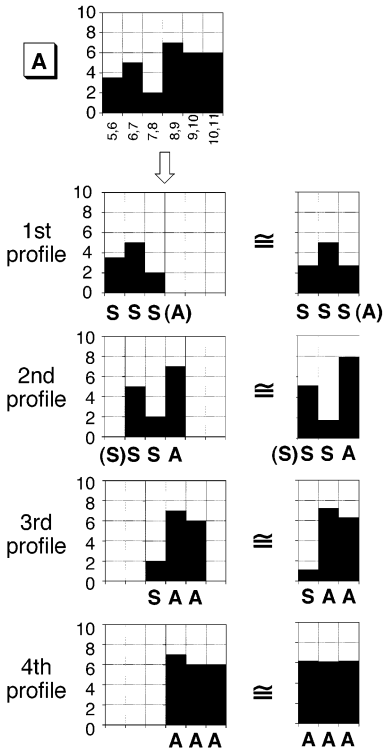

[a] The $^3J_{H,H}$ profile of 4a (Panel A) is imaginarily disected into the four small $^3J_{H,H}$ profiles and each of them is compared with the $^3J_{H,H}$ profiles composed of three contiguous spin-coupling constants. The *x* and *y* axes represent proton numbers and $^3J_{H,H}$'s (Hz), with indication of their relative stereochemistry, i.e., A = *anti* and S = *syn*.

delightfully found the resultant profiles to perfectly match the $^3J_{H,H}$ profiles listed in Chart 18.

A structural array of contiguous polyols is contained in a number of natural products, including the butyrolactols,[24] the zooxanthellatoxins,[25] the palytoxins,[1,26] the prymnesins,[27] the aflastatins,[28] the blasticidins,[29] and others. Using the NMR database discussed in this paper, we have studied their relative

(23) For the reported ^{1}H chemical shift and $^3J_{H,H}$'s of hexa- and hepta-alditol in D_2O, see: (a) Hawkes. S. E.; Lewis, D. *J. Chem. Soc., Perkin Trans. 2* **1984**, 2073−2078. (b) Gillies, D. G.; Lewis, D. *J. Chem. Soc., Perkin Trans. 2* **1985**, 1155−1159. (c) Lewis, D. *J. Chem. Soc., Perkin Trans. 2* **1986**, 467−470. (d) Angyal, S. J.; Sanders, J. K.; Grainger, C. T.; Le Fur, R.; Williams. P. G. *Carbohydr. Res.* **1986**, *150*, 7−21. (e) Lewis, D.; Angyal, S. J. *J. Chem. Soc., Perkin Trans. 2* **1989**, 1763−1765. (f) Franks, F.; Dabok, J.; Ying, S.; Kay, R. L.; Grigeera, J. R. *J. Chem. Soc., Perkin Trans. 1* **1991**, *87*, 579−585.

(24) Kotake, C.; Yamasaki, T.; Moriyama, T.; Shinoda, M.; Komiyama, N.; Furumai, T.; Konishi, M.; Oki, T. *J. Antibiot.* **1992**, *45*, 1442−1450.

(25) (a) Nakamura, H.; Asari, T.; Ohizumi, Y.; Kobayashi, J.; Yamasu, T.; Murai, A. *Toxicon* **1993**, *31*, 371−376. (b) Nakamura, H.; Asari, T.; Murai, A. *J. Am. Chem. Soc.* **1995**, *117*, 550−551. (c) Nakamura, H.; Maruyama, K.; Fujimaki, K.; Murai, A. *Tetrahedron Lett.* **2000**, *41*, 1927−1930 and references therein. For a related marine natural product zooxanthellamide A, see: (d) Onodera, K.; Nakamura, H.; Oba, Y.; Ojika, M. *Tetrahedron* **2003**, *59*, 1067−1071.

(26) For the complete NMR assignment, see: Kan, Y.; Uemura, D.; Hirata, Y.; Ishiguro, M.; Iwashita, T. *Tetrahedron Lett.* **2001**, *42*, 3197−3202.

(27) (a) Igarashi, T.; Satake, M.; Yasumoto, T. *J. Am. Chem. Soc.* **1996**, *118*, 479−480. (b) Igarashi, T.; Satake, M.; Yasumoto, T. *J. Am. Chem. Soc.* **1999**, *121*, 8499−8511. (c) Sasaki, M.; Shida, T.; Tachibana, K. *Tetrahedron Lett.* **2001**, *42*, 5725−5728 and references therein.

(28) (a) Sakuda, S.; Ono, M.; Furihata, K.; Nakayama, J.; Suzuki, A.; Isogai, A. *J. Am. Chem. Soc.* **1996**, *118*, 7855−7856. (b) Ikeda, H.; Matsumori, N.; Ono, M.; Suzuki, A.; Isogai, A.; Nagasawa, H.; Sakuda, S. *J. Org. Chem.* **2000**, *65*, 438−444, and references therein.

(29) (a) Sakuda, S.; Ono, M.; Ikeda, H.; Inagaki, Y.; Nakayama, J.; Suzuki, A.; Isogai, A. *Tetrahedron. Lett.* **1997**, *38*, 7399−7402. (b) Sakuda, S.; Ikeda, H.; Nakamura, T.; Kawachi, R.; Kondo, T.; Ono, M.; Sakurada, M.; Inagaki, H.; Ito, R.; Nagasawa, H. *J. Antibiot.* **2000**, *53*, 1378−1384 and references therein.

stereochemistry, which have given several interesting results. Among them, we should comment specifically on the relative stereochemistry proposed for the C27∼C31 portion of the aflastatins. Upon comparison of the reported spin-coupling constants with the adjacent or three contiguous $^3J_{H,H}$ profiles, it immediately becomes evident that the reported relative stereochemistry at C27∼C31 must be revised from *syn/syn/syn/syn*[28] to *anti/syn/syn/syn*.[30] Similarly, the relative stereochemistry at C25∼C29 of the blasticidins can be suggested as *anti/syn/syn/syn*.[30]

Conclusion

Using 1,2,3-triols **1a**∼**d**, 1,2,3,4-tetraols **2a**∼**h**, and 1,2,3,4,5-pentaols **3a**∼**p**, we created the $^3J_{H,H}$ databases, as well as the ^{13}C, ^1H, and $^1H(OH)$ chemical shift databases, for contiguous polyols. The fact that each diastereomer of **1a**∼**d**, **2a**∼**h**, and **3a**∼**p** exhibits a distinct and differing profile in all the ^{13}C, ^1H, $^1H(OH)$ and $^3J_{H,H}$ NMR databases argues for their usefulness for stereochemical analysis of unknown compounds bearing these structural motifs.

To systematically assess their relative values, a case study was conducted on heptaols **4a**∼**d**, through which the γ- and δ-effects were recognized, to refine the ^{13}C chemical shift profile predicted via an application of the concept of self-contained nature. Interestingly, the magnitudes of γ- and δ-effects were found to depend on a specific stereochemical arrangement of the functional groups present in both the inside and outside of a self-contained box. However, these effects were found significant only for the stereoisomers belonging to a specific sub-group. With the exception of the stereochemical arrangement of functional groups belonging to the specific sub-group, the γ- and δ-effects can, at least at the first order of approximation, be ignored for the stereochemical analysis of unknown compounds. However, for stereoisomers belonging to the specific sub-group, it is necessary to refine, with incorporation of the γ- and δ-effects, the profile predicted at the first order of approximation. With these procedures, it is possible to properly predict an NMR profile for unknown polyols. A parallel trend was found also for the case of ^1H chemical shift profiles.

With use of heptaols **4a**∼**d**, the values of $^3J_{H,H}$ profiles were tested. One of the key logics used in the NMR database approach is to analyze a *profile*, rather than a single data-point, to deduce the stereochemistry of an unknown compound. This logic was demonstrated to be very powerful for the analysis of $^3J_{H,H}$ profiles as well. Two methods, one using profiles consisting of three contiguous $^3J_{H,H}$ constants and the other using profiles consisting of two adjacent $^3J_{H,H}$ constants, have been developed.

Overall, among the methods discussed, an approach based on three, or two, contiguous $^3J_{H,H}$ profiles is *operationally simpler* than one based on ^{13}C and ^1H chemical shift profiles. Therefore, it has been suggested that a $^3J_{H,H}$ profile be used as the primary device for predicting the stereochemistry of unknown polyols and ^{13}C and ^1H chemical shift profiles be used as the secondary devices to confirm the predicted stereochemistry.

Experimental Section

The ^1H and ^{13}C NMR spectra were recorded on a Varian Inova 500 spectrometer and a Mercury 400 spectrometer, respectively. The central residual solvent-signal [^1H NMR spectrum: 3.30 ppm (CD_3OD) and 2.49 ppm (DMSO-d_6); ^{13}C NMR spectrum: 49.0 ppm (CD_3OD) and 39.5 ppm (DMSO-d_6)] was used as the internal reference. For ^1H NMR spectra in C_5D_5N, the most upfield residual solvent-signal (7.19 ppm) was used as the internal reference. For ^1H and ^{13}C NMR spectra in D_2O, the residual solvent-signal of C_6D_6 in a WILMAD coaxial insert (WGS-5BL, 50 mm L × 2 mm stem o.d.) was used as the external reference (^1H NMR spectrum: 7.15 ppm; ^{13}C NMR spectrum: 128.0 ppm). The apparent vicinal $^1H/^1H$ spin-coupling constants were obtained from 1D ^1H NMR spectra.

The synthesis of **1a**∼**d**, **2a**∼**h**, **3a**∼**p**, and **4a**∼**d**, the raw NMR data, the NMR profiles, the predicted profiles, and the stereochemical predictions of **4a**∼**d** are included in the Supporting Information.

Acknowledgment. Financial support from the National Institutes of Health (NS 12108) is gratefully acknowledged. S.H. and W.C. greatly thank a postdoctoral fellowship from the Naito Foundation and the Swiss National Science Foundation, respectively.

Supporting Information Available: The synthesis of **1a**∼**d**, **2a**∼**h**, **3a**∼**p**, and **4a**∼**d**, the raw NMR data, the NMR profiles, the predicted profiles, and the stereochemical predictions of **4a**∼**d** are included in Supporting Information (50 pages, print/PDF). This material is available free of charge via the Internet at http://pubs.acs.org.

JA0375481

(30) Higashibayashi, S.; Kobayashi, Y.; Zeng, H.; Kishi, Y. unpublished work.